Solution Structure of the Lewis x Oligosaccharide Determined by NMR Spectroscopy and Molecular Dynamics Simulations†

Kristine E. Miller, Chaitali Mukhopadhyay, Perseveranda Cagas, and C. Allen Bush*

Department of Chemistry & Biochemistry, University of Maryland Baltimore County, Baltimore, Maryland 21228, and Center of Marine Biotechnology, 600 East Lombard Street, Baltimore, Maryland 21202

Received October 25, 1991; Revised Manuscript Received May 4, 1992

ABSTRACT: The Lewis x (Le^x) determinant is a trisaccharide fragment that has been implicated as a specific differentiation antigen, as a tumor antigen, and as a key component of the ligand for the endothelial leukocyte adhesion molecule, ELAM-1. High-resolution nuclear magnetic resonance spectroscopy shows it to have a relatively rigid structure. Only a small range of glycosidic dihedral angles in the trisaccharide produce simulated nuclear Overhauser effect spectra agreeing with data measured for the human milk pentasaccharide, lacto-*N*-fucopentaose-3, which contains the Le^x determinant. Independently, the same average structure for the Le^x determinant arises from in vacuo molecular dynamics simulations. The proposed conformation of the Le^x trisaccharide is very similar to that recently determined for the closely related Le^a trisaccharide. In agreement with the recent finding that both sialylated Le^a and Le^x react with ELAM-1, the results presented here show that the Le^a and Le^x determinants contain very similar carbohydrate domains.

The Lewis x (Le^x)[1] structure (Hakomori et al., 1981) is an antigenic determinant present in a variety of normal and malignant human tissues (Knowles et al., 1982; Fox et al., 1983; Gooi et al., 1983). It may therefore be a normal component in one cell type and a tumor-associated antigen in another (Feizi, 1985). The Le^x moiety can be expressed in both glycolipid and glycoprotein molecules of a cell (Urdal et al., 1983). Also known as stage-specific embryonic antigen-1 (SSEA-1) (Solter & Knowles, 1978) and myeloid-specific antigen (My-1) (Civin et al., 1981), the Le^x determinant is a trisaccharide unit of lacto-*N*-fucopentaose-3 (LNF-3) (Kobata & Ginsburg, 1969) having the carbohydrate sequence, Galβ(1→4)[Fucα(1→3)]GlcNAcβ.

While the precise physiological role of the Le^x antigen is still unknown, some insight has been gained with respect to its biological activity. Studies have shown that expression of the Le^x antigen varies greatly during the maturation of normal human cells (Fukushima et al., 1984). As such, this carbohydrate determinant is believed to play a role in normal cell development and differentiation (Solter & Knowles, 1978; Hakomori, 1981). In addition, since many human cancer tissues accumulate this antigen (Yang & Hakomori, 1971; Hakomori et al., 1984), the Le^x determinant is presumably associated with the growth of malignant cells. Lastly, it has been suggested that the Le^x determinant may function as a recognition structure for endogenous receptors such as the lectins (Gooi et al., 1981), a class of proteins of nonimmune origin that are widely distributed in human tissues and that bind carbohydrates specifically and noncovalently. In fact, it has been recently proposed (Lowe et al., 1990; Phillips et al., 1990; Walz et al., 1990; Tiemeyer et al., 1991) that the sialylated derivative of the Le^x structure, Neu5Acα(2→3)-Galβ(1→4)[Fucα(1→3)]GlcNAcβ, is a ligand for endothelial leukocyte adhesion molecule (ELAM-1) (Bevilacqua et al., 1987), a selectin with an N-terminal lectin domain. ELAM-1 is transiently expressed on the surface of endothelial cells at sites of acute inflammation (Cotran et al., 1986; Bevilacqua et al., 1989). Hence, in addition to its function in cell regulation, there is evidence that the Le^x determinant may play a role in the inflammatory response.

Since the Le^x determinant is believed to be of pathologic importance, knowledge of its structure may be useful in predicting its bioactive conformation, interpreting its binding specificity with different receptors, designing drugs to act as inhibitors of the binding and activity of Le^x, and aiding in the structure determination of related antigenic carbohydrates. In this report we present the three-dimensional solution structure of the Le^x trisaccharide determined by two independent techniques. One approach is based on a comparison of experimental nuclear magnetic resonance (NMR) spectroscopic data recorded for the pentasaccharide LNF-3 (which contains the Le^x trisaccharide) with spectroscopic data calculated for the Le^x moiety as a function of its glycosidic conformational regime. In contrast, the second approach utilized conformational energy calculations and molecular dynamics (MD) simulations of the Le^x determinant as a means to identify the stable conformation of this oligosaccharide. Both techniques yield the same average structure for the Le^x trisaccharide.

MATERIALS AND METHODS

LNF-3, Galβ(1→4)[Fucα(1→3)]GlcNAcβ(1→3)Galβ-(1→4)Glc, was purchased from Oxford Glycosystems. An 8-mg sample of LNF-3 was exchanged in ^2H_2O and lyophilized for three cycles before final dissolution in 450 μL of high-purity ^2H_2O (99.96%; Merck, Sharp and Dohme). NMR experiments were performed on a General Electric GN-500 NMR spectrometer operating at 500.11 MHz for ^1H (125.76 MHz for ^{13}C). ^1H spectra were recorded at 24.0 and 5.5 °C

* Author to whom correspondence should be addressed.

† Research supported by NIH Grant GM-31449.

[1] Abbreviations: DQF-COSY, double-quantum-filtered correlation spectroscopy; ELAM-1, endothelial leukocyte adhesion molecule; Fuc, L-fucose; Gal, D-galactose; Glc, D-glucose; GlcNAc, *N*-acetyl-β-D-glucosamine; HMQC, heteronuclear multiple-quantum correlation; HOHAHA, homonuclear Hartmann–Hahn; Le^x, Lewis x; LNF-3, lacto-*N*-fucopentaose-3; MD, molecular dynamics; My-1, myeloid-specific antigen; Neu5Ac, *N*-acetylneuraminic acid; NMR, nuclear magnetic resonance; NOE, nuclear Overhauser effect; NOESY, nuclear Overhauser enhancement spectroscopy; SSEA-1, stage-specific embryonic antigen-1; τ_c, rotational correlation time; T_1, spin–lattice relaxation time.

0006-2960/92/0431-6703$03.00/0

with a spectral width of 2.4 kHz and 4K complex data points, and broad-band ^{1}H-decoupled ^{13}C spectra were obtained at 25.0 °C with a 25-kHz spectral width and 8K complex data points. One-dimensional nonselective and selective ^{1}H spin–lattice relaxation time (T_1) experiments and two-dimensional DQF-COSY, HOHAHA, NOESY, and HMQC experiments were conducted as previously described (Cagas & Bush, 1990). These latter experiments were performed at 24.0 °C, except the NOESY experiment which was conducted at 5.5 °C with a mixing time of 250 ms. The ^{1}H and ^{13}C chemical shifts were measured with respect to internal acetone at 2.225 and 31.07 ppm, respectively. NMR data were processed and NOESY cross peaks were evaluated quantitatively, as recently reported (Cagas & Bush, 1990), by using the FTNMR program[2] on a Silicon Graphics 4D/35 workstation.

NOESY spectra for a particular mixing time τ_m can be calculated according to the complete relaxation matrix method (Keepers & James, 1984). In this study, NOE cross peak intensities and nonselective ^{1}H T_1 values were simulated using the software SIMNOE. This program is a modified version of that described previously (Cagas & Bush, 1990) wherein a matrix of relaxation rates is built for a three-dimensional structural model. The matrix is subsequently diagonalized, and the eigenvalues and eigenvectors are determined by the Givens method using QCPE program 62 (Prosser, 1965). Nonselective ^{1}H T_1 values are calculated directly from the elements of the relaxation rate matrix, while NOE diagonal and cross peak intensities are derived from the eigenvectors and eigenvalues of the diagonalized matrix. The method used assumes an isotropically rotating molecule in a single rigid conformation. Although this assumption is a significant one, which must be validated, it is subject to testing within our method by the possibility that no single conformation can be found which agrees with the experimental NOE data. In this methodology, τ_c is adjusted to fit cross peaks, such as those on a single pyranoside residue, that do not depend strongly on conformation. The three-dimensional conformational models utilized by SIMNOE are generated using CHARMm.[3] Implementation of this approach required relinking CHARMm so that it would call on SIMNOE as an external program. In practice, a series of conformers is generated for a molecule by systematically changing the value of one or more dihedral angles. Each time a new conformer is generated by CHARMm, its coordinates are written to an external file and then SIMNOE is called upon to read the external file and execute. Once SIMNOE has completed its computations, the results are saved and control is returned to CHARMm, which proceeds to generate the next conformational model.

Simulation of the cross peak intensities and nonselective T_1 values of the Le^x trisaccharide, Galβ(1→4)[Fucα(1→3)]-GlcNAcβ-OMe, was conducted as follows. Preliminary models for the two disaccharide components, Galβ(1→4)-GlcNAcβ-OMe and Fucα(1→3)GlcNAcβ-OMe, of Le^x were constructed from monosaccharide templates. Disaccharide conformations were then generated by systematically varying the ϕ and ψ glycosidic dihedral angles from 0° to 350° by 10° angle increments, and the corresponding NOESY spectra were simulated for each model. The dihedral angle ranges in the disaccharide conformers that had calculated NOEs between the anomeric and aglycon protons that agreed with the corresponding experimental values for LNF-3 were recorded. Finally, conformations of the Le^x trisaccharide were generated by allowing the four glycosidic dihedral angles to adopt all values within 10° increments in the previously recorded angle ranges, and the NOESY spectrum and nonselective ^{1}H T_1 values were simulated for each conformational model. Conformers with calculated interresidue NOEs and nonselective ^{1}H T_1 values in agreement with experimental data for LNF-3 were stored.

Lastly, independent from the NOESY experiments and simulations described above, conformational energy calculations and MD simulations for the Le^x trisaccharide were conducted using CHARMm with the force field developed for carbohydrates by Rasmussen and co-workers (Rasmussen, 1982). This parameter set is most suitable for calculations without explicit inclusion of solvent and has been previously reported for a number of MD simulations of monosaccharides and oligosaccharides (Mukhopadhyay & Bush, 1991; Brady, 1986, 1987, 1990; Carver et al., 1990; Yan & Bush, 1990). Conformational energy maps[4] were calculated for rigid rotations around the glycosidic linkages of each of the disaccharide components of the Le^x trisaccharide. These calculations were performed by systematically varying each of the glycosidic dihedral angles from 0° to 350° by 10° angle increments. The corresponding relaxed conformational energy maps were subsequently generated by relaxing all degrees of freedom, except the glycosidic dihedral angles, via energy minimization. Each disaccharide conformation within 5 kcal/mol of the minimum energy conformation was then subjected to further energy minimization (i.e., completely relaxed), and the resulting structures were used to construct preliminary structural models of the Le^x trisaccharide. Energy minimization of these trisaccharide conformations led to two closely related energy minima, A and B. Lastly, two MD simulations, MD1 and MD2, of the Le^x trisaccharide were performed using the two energy minima A and B as initial structures. Trajectories of 300 ps were generated by methods similar to those reported in earlier studies from this laboratory (Mukhopadhyay & Bush, 1991; Yan & Bush, 1990).

RESULTS

By use of a combination of homonuclear and heteronuclear two-dimensional NMR techniques, the ^{1}H and ^{13}C spectra of LNF-3 were completely assigned. The ^{1}H resonances of LNF-3 were assigned by standard methods that rely on correlation through chemical bonds. Correlation by double-quantum-filtered correlation spectroscopy (DQF-COSY) (Piantini et al., 1982; Shaka & Freeman, 1983; Rance et al., 1983) of the signals assigned to vicinal protons was initiated at the anomeric resonances. Cross peaks were analyzed to give multiplet shapes, and the stereochemistry of each sugar was assigned from approximate values of the coupling constants, $^3J_{HH}$ (Altona & Hasnoot, 1980; Hasnoot et al., 1980; Koerner et al., 1983; Bush, 1988). In the case of strongly coupled ^{1}H signals, for which cross peaks lie close to the diagonal, the homonuclear Hartmann–Hahn (HOHAHA) (Braunschweiler & Ernst, 1983; Davis & Bax, 1985; Bax & Davis, 1985) spectrum provided additional information on the assignment. The ^{1}H-detected ^{13}C heteronuclear multiple-quantum correlation (HMQC) (Muller, 1979; Bax et al., 1983; Bendall et al., 1983) experiment further resolved any cases of overlapping resonances by providing accurate values of chemical shifts for strongly coupled ^{1}H resonances (Abeygunawardana et al., 1990).

Complete assignment of the ^{1}H resonances of LNF-3, given in Table I, is important in order to avoid misinterpretation of a cross peak in the nuclear Overhauser enhancement spec-

[2] Hare Research, Inc., 14810 216th Ave. NE, Woodinville, WA 98072.
[3] Polygen Corp., 200 Fifth Ave., Waltham, MA 02254.
[4] Ramachandran-like contour maps of the conformational potential energy as a function of the glycosidic dihedral angles.

Table I: ^{1}H NMR Chemical Shifts[a] of LNF-3

residue[b]	H1	H2	H3	H4	H5	H61, H62	NAc[c]
αGlc	5.220	3.576	3.828	3.642	3.948	3.837, 3.889	
βGlc	4.663	3.281	3.642	3.653	3.599	3.791, 3.950	
βGal$^{4'}$	4.436	3.578	3.712	4.156	3.708	3.737, 3.769	
βGlcNAc^3	4.715	3.967	3.882	3.957	3.578	3.870, 3.969	2.023
αFuc^3	5.128	3.692	3.908	3.793	4.837	1.178	
βGal^4	4.464	3.497	3.654	3.901	3.602	3.746, 3.793	

[a] Chemical shifts are referenced against internal acetone at 2.225 ppm. Accuracy is ±0.005 ppm. [b] A superscript at the name of a sugar residue indicates to which position of the adjacent monosaccharide it is glycosidically linked; e.g., αFuc^3 means Fuc is α(1→3) linked to GlcNAc. βGal^4 refers to the nonreducing terminal of LNF-3. [c] NAc refers to the methyl protons of an acetamido group.

Table II: ^{13}C NMR Chemical Shifts[a] of LNF-3

residue[b]	C1	C2	C3	C4	C5	C6	NAc[c]
αGlc	92.68	72.00	72.27	79.23	70.99	60.83	
βGlc	96.61	74.66	75.23	79.14	75.67[d]	60.96	
βGal$^{4'}$	103.78	70.85	82.93	69.21	75.79	62.37	
βGlcNAc^3	103.40	56.84	75.62	73.94	76.00	60.51	175.57, 23.13
αFuc^3	99.47	68.58	70.07	72.78	67.56	16.18	
βGal^4	102.65	71.93	73.35	69.21	75.74[d]	61.84	

[a] Chemical shifts are referenced against internal acetone at 31.07 ppm. Although the C–H connectivities were established by ^{1}H[^{13}C] HMQC (±0.1 ppm), accurate chemical shifts (±0.02 ppm) were obtained from the ^{13}C spectrum at 125 MHz. [b] For naming of sugar residues, see footnotes to Table I. [c] NAc refers to the carbonyl and methyl carbons of an acetamido group. [d] These assignments may be interchanged.

troscopy (NOESY) spectrum. The ^{1}H assignments reported here differ in several respects from those reported earlier (Breg et al., 1988). For example, the assignments published previously were incomplete in the sense that no chemical shift was determined for the βGal^4 H5 proton, and with the exception of the αFuc^3 H6 proton, an assignment of the H6 signals was lacking. In addition, six of the ^{1}H chemical shifts reported here differ by more than experimental error[5] from the values reported by Breg et al. Specifically, the values we report for βGlcNAc^3 H4 and βGal^4 H3 differ significantly (by 0.340 and 0.303 ppm, respectively) from those in the Breg paper, while those for βGlc H3, αGlc H5, αFuc H3, and βGlcNAc H5 differ to a lesser extent (0.010–0.030 ppm). Significantly, the value reported by Breg et al., for Gal^4 H3 (3.956 ppm) agrees within experimental error with the assignment we provide for GlcNAc H4, while the Breg assignment for GlcNAc H4 (3.627 ppm) only differs by 0.026 ppm from the Gal^4 H3 chemical shift in Table I. There are also discrepancies between the ^{13}C assignments for LNF-3 obtained in this study and those of Breg et al. For example, only 18% of the ^{13}C resonances in Table II are within experimental error[6] of the values reported by Breg et al. This is due largely to the fact that approximately 63% of the ^{13}C chemical shifts measured in our laboratory are, on average, 0.07 ppm greater than the corresponding values measured by Breg and co-workers. However, seven of the ^{13}C assignments in the Breg article deviate significantly (by more than 0.2 ppm) from those reported here. Four of these deviations may be explained if two sets of assignments are interchanged; namely, Gal^4 C6/Gal$^{4'}$ C6 and GlcNAc C5/GlcNAc C3. In the Breg report, the H6 and H6′ protons in the sugar residues could not be recognized separately and so the average chemical shift of both protons was reported in some cases. In this study, the H6 protons of all the residues are clearly resolved in the HMQC spectrum (Figure 1), which shows that the average chemical shifts for the two H6's in Gal^4 and Gal$^{4'}$ are 3.769 and 3.753 ppm, respectively (see Table II). The three remaining discrepancies are Gal$^{4'}$ C5, GlcNAc C4, and Gal^4 C3. Analogous to the discussion above regarding the ^{1}H assignments, the value reported by Breg et al. for Gal^4 C3 (73.88 ppm) agrees with the assignment we provide for GlcNAc C4. However, the Breg assignment for GlcNAc C4 (73.14 ppm) differs by 0.21 ppm from the Gal^4 C3 chemical shift in Table II.

Quantitative NOEs were obtained through calibration of cross peak magnitudes in the NOESY (Jeener et al., 1979; Kumar et al., 1980; States et al., 1982) spectrum shown in Figure 2. Large negative NOE cross peaks between protons in the same residue were used to calibrate the rotational correlation time, τ_c.[7] Additional cross peaks were observed between the anomeric and aglycon protons as well as between protons in residues not directly bonded. Cross peak volumes in Table IIIA are expressed as the percent of the volume of a diagonal peak of a single proton at zero mixing time. The volume of an isolated diagonal peak at zero mixing time is calculated from its volume at a nonzero mixing time (τ_m = 250 ms in this study) and from the selective ^{1}H T_1 for that peak. This type of cross peak normalization is appropriate in cases where data from a single NOESY experiment are used to quantitatively evaluate cross peak volumes (Mirau, 1988; Mirau & Bovey, 1986). Experimentally measured nonselective ^{1}H T_1 values are reported in Table IIIB.

NOE and nonselective ^{1}H T_1 values were simulated from conformational models of the Le^x trisaccharide. Figure 3 illustrates the simulated NOEs as a function of conformation of each glycosidic linkage in the Le^x trisaccharide. It can be seen from this figure that although a large number of ϕ and ψ combinations yield the NOE intensity observed between the hydrogens across the glycosidic linkages, fewer yield the experimental NOE values observed between protons on residues not directly bonded to each other and still fewer yield the nonselective ^{1}H T_1 values. The glycosidic dihedral angles of the conformations that are consistent with experimental NOE and nonselective ^{1}H T_1 values are reported in Table IV.

Independently, two energy minima, A and B, were identified from conformational energy calculations of the Le^x trisac-

[5] The combined experimental error in the ^{1}H assignments of our study (±0.005 ppm) and that of Breg et al. (1988) (±0.003 ppm) is ± 0.008 ppm.

[6] The combined experimental error in the ^{13}C assignments of our study (±0.02 ppm) and that of Breg et al. (1988) (±0.02 ppm) is ± 0.04 ppm.

[7] For LNF-3 in ^2H_2O at 5.5 °C, τ_c was estimated to be 0.83 ± 0.09 ns.

[8] IUPAC and IUB Joint Commission on Biochemical Nomenclature (1983) *Pure Appl. Chem. 55*, 1269.

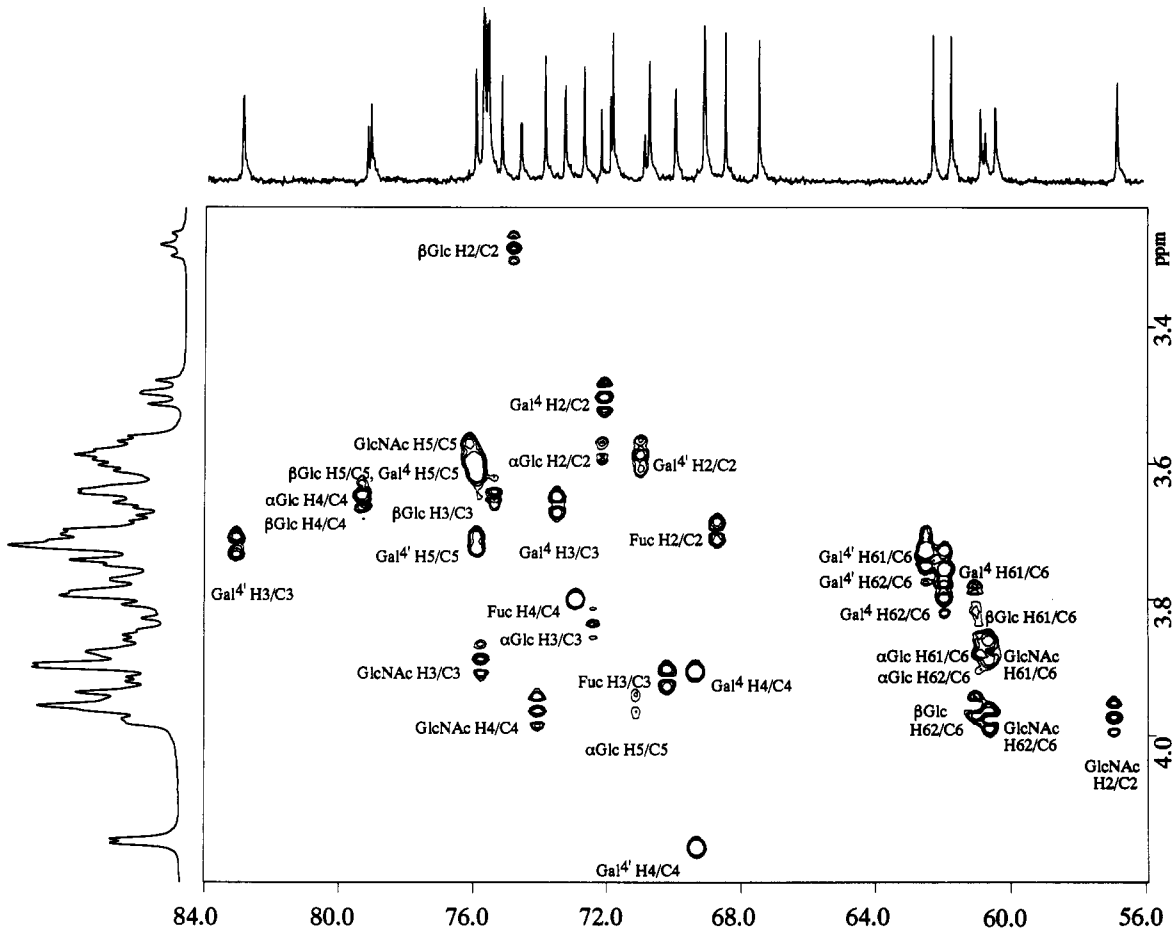

FIGURE 1: Phase-sensitive ^{13}C-decoupled, ^{1}H-detected multiple-quantum correlation ($^{1}H[^{13}C]$ HMQC) spectrum of LNF-3 recorded at 500-MHz proton frequency. The data matrix was 2 × 256 × 1K complex points with 64 scans per t_1 value. The spectral window was 2403.84 Hz in the F_1 dimension and 12500.00 Hz in the F_2 dimension. Sine bell apodization with 45° and 90° phase shifts was used in the t_2 and t_1 dimensions, respectively. Data were zero filled in the t_1 dimension to obtain a 1K × 1K real matrix with digital resolution of ±0.005 (^{1}H) and ± 0.1 ppm/point (^{13}C). Portions of the 1D ^{1}H and ^{13}C spectra of LNF-3 are displayed at the left and the top, respectively.

charide. Conformers A and B are structurally very similar (see Table IV), differing mainly in the value of ϕ_2, the dihedral angle for the $\alpha(1\rightarrow3)$ linkage. Significantly, these two conformations differ by only ~0.7 kcal/mol in energy. In a previous study (Thogersen et al., 1982), a minimum energy conformation for the Le^x trisaccharide was reported with the following dihedral angles: $\phi_1 = -65°$, $\psi_1 = 130°$, $\phi_2 = -65°$, and $\psi_2 = -95°$. This structure was determined by performing rigid conformational energy mapping (i.e., the energy value was calculated at each grid point in the conformational space without having performed energy minimization) using the HSEA[9] force field. While the ϕ_1, ψ_1, and ψ_2 values of this structure are in good agreement with those of conformers A and B, the ϕ_2 dihedral angle value in the Thogersen structure is different from that in both of the minimum energy conformers reported in this study. In fact, the Le^x conformation reported by Thogersen et al. is very similar to the average structures resulting from MD simulations of conformers A and B (see MD1 and MD2 in Table IV).

After thermal equilibration, data gathered over 300 ps illustrated that the trajectories in the MD simulations were quite stable. Table IV reports the fluctuation in the glycosidic dihedral angles resulting from MD simulations of conformers A and B, and Figure 4 shows the time series of the glycosidic dihedral angles over 300 ps obtained for conformer A. Overall, the data show that nearly identical trajectories were found for both starting conformations (Table IV). Similar to our results on other blood group oligosaccharides (Mukhopadhyay & Bush, 1991; Yan & Bush, 1990), fluctuations of the glycosidic dihedral angles on the order of ±10° were observed on a 1-ps time scale. Notably, Figure 4C shows that the dihedral angle, ϕ_2, fluctuates significantly more than the other three glycosidic dihedral angles (ϕ_1, ψ_1, ψ_2). These data are consistent with transitions between the two closely related energy minima separated by a low-energy barrier.

DISCUSSION

The average structure of the Le^x trisaccharide has been determined by two independent techniques. The results of NOE and nonselective ^{1}H T_1 simulation for the Le^x determinant show (Table IV) that only a small group of closely related conformers is consistent with the experimental data measured for the pentasaccharide LNF-3. We believe this pentasaccharide to be a good model for the Le^x trisaccharide. Evidence that the reducing terminal lactose function does not interact with the Le^x determinant includes absence of NOE between these two parts of the pentasaccharide and molecular models which show the two parts of the pentasaccharide to be well separated. While the data presented here do not rigorously prove that the Le^x trisaccharide has a single unique conformation, they identify a very narrowly defined conformational manifold for the Le^x glycosidic linkages. In addition to the data derived from NOE and ^{1}H T_1 simulations, data from MD simulations are also presented in Table IV. The

[9] The HSEA force field is not fully parameterized. It contains only a van der Waals potential and a torsional potential term called "exoanomeric effect".

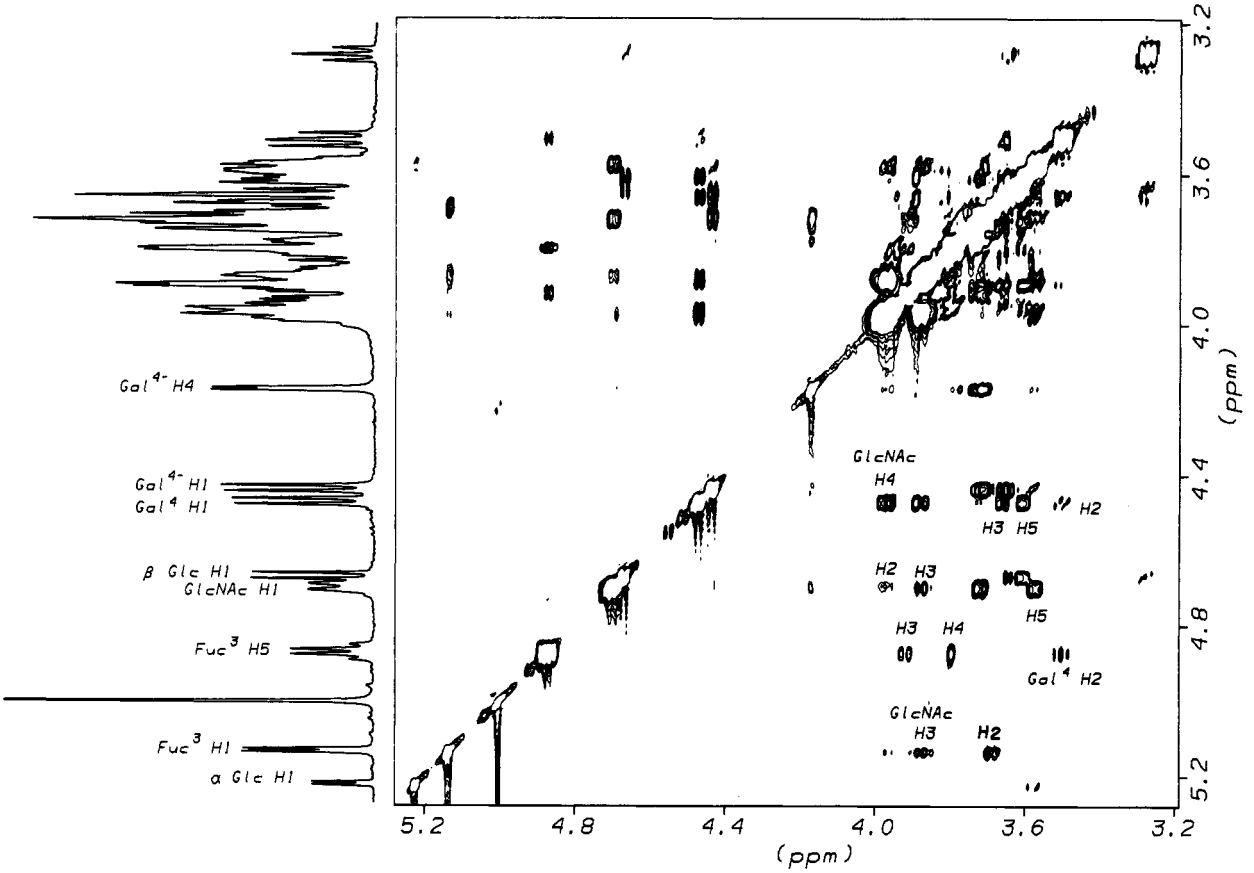

FIGURE 2: 2D NOESY spectrum of LNF-3 at 500 MHz. The data matrix was 2 × 256 × 1K complex points with 32 scans per t_1 value and a 250-ms mixing time. The spectral window was 2403.84 Hz. Sine bell apodization with 45° and 90° phase shifts was used in the t_2 and t_1 dimensions, respectively. Data were zero filled in the t_1 dimension to obtain a 1K × 1K real matrix with digital resolution of ±0.005 ppm/point. Part of the ^{1}H 1D spectrum of LNF-3 is displayed at the left. The labeled cross peaks correspond to the intra-and interresidue cross peaks reported in Table IIIA.

Table III: Experimental Normalized NOESY Cross Peak Intensities and Nonselective ^{1}H T_1 Values for LNF-3

A. Normalized NOESY Cross Peak Intensities[a]

cross peak[b]	% NOE[c]	cross peak[b]	% NOE[c]
αFuc^3 H1/H2	4.4 (±1)	βGal^4 H1/H3	3.2 (±1)
αFuc^3 H3/H5	2.7 (±1)	βGal^4 H1/H5	5.1 (±1)
αFuc^3 H4/H5	4.0 (±1)	αFuc^3 H1/βGlcNAc^3 H3	2.8 (±1)
βGlcNAc^3 H1/H3	3.2 (±1)	βGal^4 H1/βGlcNAc^3 H4	5.6 (±1)
βGlcNAc^3 H1/H5	6.2 (±1)	αFuc^3 H5/βGal^4 H2	2.4 (±1)

B. Nonselective ^{1}H T_1

resonance	T_1[d] (s)	resonance	T_1[d] (s)
αFuc^3 H1	2.06 (±0.03)	βGal^4 H1	1.07 (±0.03)
αFuc^3 H5	0.98 (±0.03)	βGal^4 H2	1.59 (±0.03)

[a] Intraresidue NOESY cross peak intensities, which were used to calibrate τ_c, and interresidue NOESY cross peak intensities, which were used in the NOESY simulations. [b] For naming of the sugar residues, see footnotes to Table I. [c] Cross peak volume expressed as the percent of the volume of a diagonal peak of a single proton at zero mixing time: [(cross peak volume at τ_m = 250 ms)/(diagonal peak volume of a single proton at τ_m = 0 ms)] × 100. The denominator is calculated from the volume of an isolated diagonal peak at a mixing time of 250 ms and from the corresponding selective ^{1}H spin–lattice relaxation time (Freeman et al., 1974; Mirau, 1988), both of which were measured under identical experimental conditions. [d] Nonselective ^{1}H spin–lattice relaxation times (Cutnell et al., 1976; Freeman et al., 1980).

latter were generated using two minimum energy conformers, A and B, as starting structures. These two conformers of the Le^x determinant are extremely similar, both structurally and energetically. Indeed, the MD simulations (MD1 and MD2) of conformers A and B illustrate that, during the course of a 300-ps trajectory, the two minimum energy conformers assume essentially the same average structure. In addition, the root-mean-square fluctuations of the glycosidic dihedral angles in both MD simulations are generally ±10°, with the exception of ϕ_2, where they are ±20°. These results suggest that, overall, the glycosidic linkages of the Le^x trisaccharide have limited flexibility.

A comparison of the results obtained from the NOE simulation and the conformational energy calculations shows (Table IV) that one of the minima (conformer A) corresponds to the conformational range obtained from the NOE simulation, while the other conformer (conformer B) does not. Although the MD trajectory (Figure 4) visits both of the minima in vacuum, their relative populations could presumably be influenced by inaccuracies in the force field parameters and lack of inclusion of explicit solvent molecules in the MD calculations. Similarly, our treatment of NOE and ^{1}H T_1 simulations is not completely rigorous and should not be overinterpreted. In particular, the methodology employed in this study identifies static structures whose calculated NOE intensities are in agreement with the experimental NOE intensities. This approach does not allow for the presence of multiple solution conformations. Indeed, implementation of procedures for obtaining solution structures from NOE data that accommodate multiple conformations is not straightforward [Landis and Allured (1991), and references therein]. Overall, the results of the NOE and MD simulations presented here indicate that the conformational regime for the Le^x trisaccharide is quite narrow. Specifically, the MD trajectories illustrate that this oligosaccharide resides in two local minima that are very close to one another on the potential energy surface. In summary, we conclude that the Le^x determinant

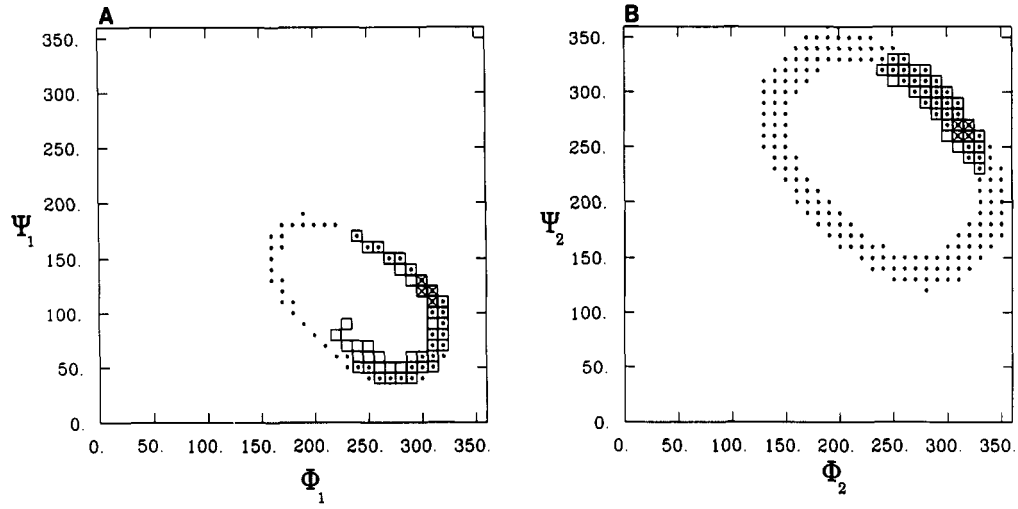

FIGURE 3: Maps of simulated NOEs as a function of conformation of each glycosidic linkage in the Le^x trisaccharide. Small circles show those values of the glycosidic dihedral angles on a 10° grid for which a conformation is found whose simulated NOEs match the experimental values within the experimental error limits given in Table IIIA of the NOEs between the anomeric and aglycon protons. Conformations for which simulated values of the remote NOE between Gal H2 and Fuc H5 also agree with experiment are indicated by a square, and the ×-marked points indicate those conformations for which the simulated nonselective ^{1}H T_1 values of Table IIIb also agree with experiment. Glycosidic dihedral angles are defined as follows with right-handed rotations representing positive dihedral angles in accordance with IUPAC recommendations:[8] ϕ_1 = (GalO5–GalC1–GalO1–GlcNAcC4), ψ_1 = (GalC1–GalO1–GlcNAcC4–GlcNAcC3), ϕ_2 = (FucO5–FucC1–FucO1–GlcNAcC3), ψ_2 = (FucC1–FucO1–GlcNAcC3–GlcNAcC2). (A) ϕ_1 vs ψ_1 for the Gal $\beta(1\rightarrow4)$ linkage. (B) ϕ_2 vs ψ_2 for the Fuc$\alpha(1\rightarrow3)$ linkage.

Table IV: Glycosidic Dihedral Angles[a] of Le^x Determinant

	ϕ_1	ψ_1	ϕ_2	ψ_2
SIMNOE[b]	−55 (±10)	120 (±15)	−45 (±10)	−95 (±10)
MD1[c]	−61 (±9)	128 (±7)	−59 (±20)	−88 (±10)
MD2[d]	−64 (±10)	128 (±8)	−64 (±21)	−88 (±11)
conformer A[e]	−57	122	−45	−96
conformer B[e]	−65	132	−83	−97

[a] Glycosidic dihedral angles are defined in the legend for Figure 3. [b] Conformations consistent with experimental NOE and nonselective T_1 values of LNF-3 (See Table III and Figure 3). [c] Average dihedral angle value (± fluctuation) resulting from a 300-ps molecular dynamics simulation of minimum energy conformer A. [d] Average dihedral angle value (± fluctuation) resulting from a 300-ps molecular dynamics simulation of minimum energy conformer B. [e] Minimum energy conformers of Le^x resulting from conformational energy calculations (see text). The energy of conformer B is 0.7 kcal/mol greater than that of conformer A.

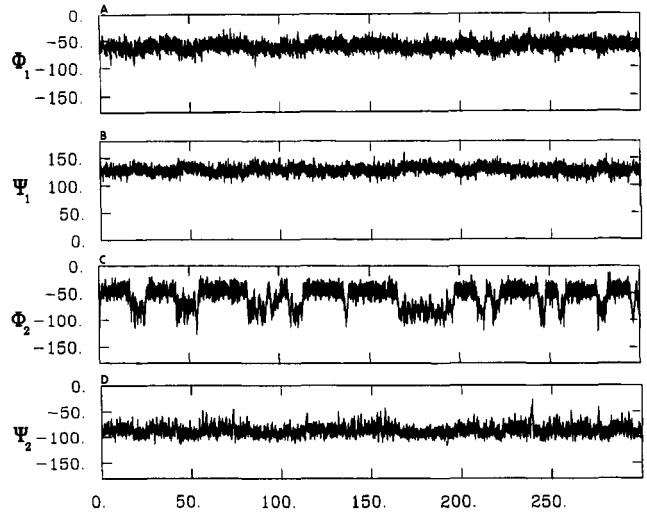

FIGURE 4: Histories of the glycosidic dihedral angles in the 300-ps molecular dynamics trajectory of conformer A of the Le^x determinant (see Table IV). (A) ϕ_1 [Gal$\beta(1\rightarrow4)$ linkage]. (B) ψ_1 [Gal$\beta(1\rightarrow4)$ linkage]. (C) ϕ_2 [Fuc$\alpha(1\rightarrow3)$ linkage]. (D) ψ_2 [Fuc$\alpha(1\rightarrow3)$ linkage].

is rigid in the sense that three of the glycosidic linkages can fluctuate over a very limited range (±10°) and the fourth may fluctuate as much as ±20°.

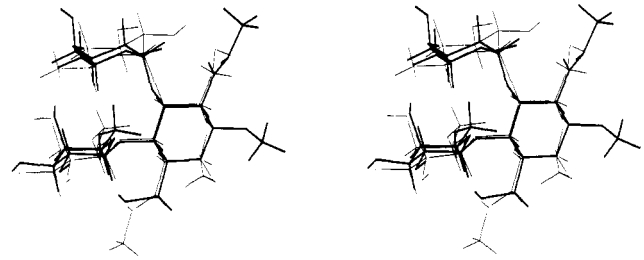

FIGURE 5: Stereoview of the Le^x trisaccharide conformer A (see Table IV), represented by bold lines, superimposed with the structural model of the Le^a trisaccharide (Cagas & Bush, 1990), Gal$\beta(1\rightarrow3)$-[Fuc$\alpha(1\rightarrow4)$]GlcNacβ–OMe.

Our finding that the Le^x trisaccharide is relatively rigid implies that it should be included in the group of comparatively inflexible blood group A, H, Le^a, and Le^b determinants previously studied in our laboratory (Bush & Cagas, 1991; Cagas et al., 1991; Cagas & Bush, 1990; Yan et al., 1987; Bush et al., 1986; Rao et al., 1985). The relationship between the Le^x and Le^a trisaccharides is shown in Figure 5 in which the Le^a structure (Cagas & Bush, 1990) is rotated by 180° about a vector normal to the C3–C4 bond of the GlcNAc ring so as to superimpose the Le^a galactose and fucose rings with those of Le^x. This figure reveals that the conformations of these two molecules are very similar with the fucose and galactose rings tightly stacked in a rigid conformation. In general, the Le^a determinant does not cross-react with the Le^x determinant although some instances have been found (Feizi, 1991). On the other hand, it has recently been reported (Berg et al., 1991; Tyrrell et al., 1991) that sialylated Le^a reacts both with ELAM-1 and with monoclonal antibodies for sialylated Le^x. The work reported here provides experimental and theoretical support for their suggestion that the molecular shapes of Le^a and Le^x may be similar. In conclusion, we suggest that receptors with which Le^a and Le^x do not cross-react must interact with functional groups other than just the fucose and galactose residues of these trisaccharides. Specifically, Figure 5 shows that the main difference in the three-dimensional structures of Le^a and Le^x lies in the orientation of the two GlcNAc rings such that the GlcNAc C2 substituent of Le^a extends into the same region of space as the GlcNAc C6 substituent of Le^x and vice versa. Thus, the C2 acetamido

and the C6 hydroxymethyl groups of the GlcNAc residues of these two trisaccharides may play a role in determining certain biological activities of Le^a and Le^x. Conversely, these two groups apparently do not interact with the receptor, ELAM-1, which fails to discriminate between the isomeric oligosaccharides. These considerations may be significant in the design of drugs to inhibit the activities of Le^x and Le^a and other related determinants.

ACKNOWLEDGMENT

We thank Hare Research for their donation of the FTNMR program.

REFERENCES

Abeygunawardana, C., Bush, C. A., & Cisar, J. O. (1990) *Biochemistry 29*, 234.

Altona, A., & Hasnoot, C. A. G. (1980) *Org. Magn. Reson. 13*, 417.

Bax, A., & Davis, D. G. (1985) *J. Magn. Reson. 65*, 355.

Bax, A., Griffey, R. H., & Hawkins, B. L. (1983) *J. Magn. Reson. 55*, 301.

Bendall, M. R., Pegg, D. T., & Doddrell, D. M. (1983) *J. Magn. Reson. 52*, 81.

Berg, E. L., Robinson, M. K., Mansson, O., Butcher, E. C., & Magnani, J. L. (1991) *J. Biol. Chem. 266*, 14869.

Bevilacqua, M. P., Pober, J. S., Mendrick, D. L., Cotran, R. S., & Gimbrone, M. A. (1987) *Proc. Natl. Acad. Sci. U.S.A. 84*, 9238.

Bevilacqua, M. P., Stengelin, S., Gimbrone, M. A., & Seed, B. (1989) *Science 243*, 1160.

Brady, J. W. (1986) *J. Am. Chem. Soc. 108*, 8153.

Brady, J. W. (1987) *Carbohydr. Res. 165*, 306.

Brady, J. W. (1990) in *Advances in Biophysical Chemistry* (Bush, C. A., Ed.) *Vol. 1*, pp 155–202, JAI Press, Greenwich, CT.

Braunschweiler, L., & Ernst, R. R. (1983) *J. Magn. Reson. 53*, 521.

Breg, J., Romijn, D., & Vliegenthart, J. F. G. (1988) *Carbohydr. Res. 183*, 19.

Bush, C. A. (1988) *Bull. Magn. Reson. 10*, 73.

Bush, C. A., & Cagas, P. (1991) in *Advances in Biophysical Chemistry* (Bush, C. A., Ed.) Vol. 2, JAI Press, Greenwich, CT (in press).

Bush, C. A., Yan, Z.-Y., & Rao, B. N. N. (1986) *J. Am. Chem. Soc. 108*, 6168.

Cagas, P., & Bush, C. A. (1990) *Biopolymers 30*, 1123.

Cagas, P., Kaluarachchi, K., & Bush, C. A. (1991) *J. Am. Chem. Soc. 113*, 6815.

Carver, J. P., Mandel, D., Michnick, S. W., Imberty, A., & Brady, J. W. (1990) in *Computer Modeling of Carbohydrate Molecules* (French, A. D., & Brady, J. W., Eds.) ACS Symposium Series 430, pp 266–280, American Chemical Society, Washington DC.

Civin, C. I., Mirro, J., & Banquerigo, M. L. (1981) *Blood 57*, 842.

Cotran, R. S., Gimbrone, M. A., Bevilacqua, M. P., Mendrick, D. L., & Pober, J. S. (1986) *J. Exp. Med. 164*, 661.

Cutnell, J. D., Bleich, H. E., & Glasel, J. A. (1976) *J. Magn. Reson. 21*, 43.

Davis, D. G., & Bax, A. (1985) *J. Am. Chem. Soc. 107*, 2820.

Feizi, T. (1985) *Nature 314*, 53.

Feizi, T. (1991) *Trends Biochem. Sci. 16*, 84.

Fox, N., Damjanov, I., Knowles, B. B., & Solter, D. (1983) *Cancer Res. 43*, 669.

Freeman, R., Hill, H. D. W., Tomlinson, B. L., & Hall, L. D. (1974) *J. Chem. Phys. 61*, 4466.

Freeman, R., Kempsell, S. P., & Levitt, M. H. (1980) *J. Magn. Reson. 38*, 453.

Fukushima, K., Hirota, M., Terasaki, P. I., Wakisaka, A., Togashi, H., Chia, D., Suyama, N., Fukushi, Y., Nudelman, E., & Hakomori, S.-I. (1984) *Cancer Res. 44*, 5279.

Gooi, H. C., Feizi, T., Kapadia, A., Knowles, B. B., Solter, D., & Evans, M. J. (1981) *Nature 292*, 156.

Gooi, H. C., Thorpe, S. J., Hounsell, E. F., Rumpold, H., Kraft, D., Forster, O., & Feizi, T. (1983) *Eur. J. Immunol. 13*, 306.

Hakomori, S.-I. (1981) *Annu. Rev. Biochem. 50*, 733.

Hakomori, S.-I., Nudelman, E., Levery, S., Solter, D., & Knowles, B. B. (1981) *Biochem. Biophys. Res. Commun. 100*, 1578.

Hakomori, S.-I., Nudelman, E., Levery, S. B., & Kannagi, R. (1984) *J. Biol. Chem. 259*, 4672.

Hasnoot, C. A. G., DeLeeuw, F. A. A. M., & Altona, C. (1980) *Tetrahedron 36*, 2783.

Jeener, J., Meier, B. H., Bachmann, P., & Ernst, R. R. (1979) *J. Chem. Phys. 71*, 4546.

Keepers, J. W., & James, T. L. (1984) *J. Magn. Res. 57*, 404.

Knowles, B. B., Rappaport, J., & Solter, D. (1982) *Dev. Biol. 93*, 54.

Kobata, A., & Ginsburg, V. (1969) *J. Biol. Chem. 244*, 5496.

Koerner, T. A. W., Jr., Prestegard, J. H., Demou, P. C., & Yu, R. K. (1983) *Biochemistry 22*, 2676.

Kumar, A., Ernst, R. R., & Wüthrich, K. (1980) *Biochem. Biophys. Res. Commun. 95*, 1.

Landis, C., & Allured, V. S. (1991) *J. Am. Chem. Soc. 113*, 9493.

Lowe, J. B., Stoolman, L. M., Nair, R. P., Larsen, R. D., Berhend, T. L., & Marks, R. M. (1990) *Cell 63*, 475.

Mirau, P. A. (1988) *J. Magn. Reson. 80*, 439.

Mirau, P. A., & Bovey, F. A. (1986) *J. Am. Chem. Soc. 108*, 5130.

Mukhopadhyay, C., & Bush, C. A. (1991) *Biopolymers 31*, 1737.

Muller, L. (1979) *J. Am. Chem. Soc. 101*, 4481.

Phillips, M. L., Nudelman, E., Gaeta, F. C. A., Perez, M., Singhal, A. K., Hakomori, S.-I., & Paulson, J. C. (1990) *Science 250*, 1130.

Piantini, U., Sorensen, O. W., & Ernst, R. R. (1982) *J. Am. Chem. Soc. 104*, 6800.

Prosser, F. (1965) *QCPE No. 11.*

Rance, M., Sorensen, O. W., Bodenhausen, G., Wagner, G., Ernst, R. R., & Wuthrich, K. (1983) *Biochem. Biophys. Res. Commun. 117*, 479.

Rao, B. N. N., Dua, V. K., & Bush, C. A. (1985) *Biopolymers 24*, 2207.

Rasmussen, K. (1982) *Acta Chem. Scand. A 36*, 323.

Shaka, A. J., & Freeman, R. (1983) *J. Magn. Reson. 51*, 169.

Solter, D., & Knowles, B. B. (1978) *Proc. Natl. Acad. Sci. U.S.A. 75*, 5565.

States, D. J., Haberkorn, R. A., & Ruben, D. J. (1982) *J. Magn. Reson. 48*, 286.

Thogersen, H., Lemieux, R. U., Bock, K., & Meyer, B. (1982) *Can. J. Chem. 60*, 44.

Tiemeyer, M., Swiedler, S. J., Ishihara, M., Moreland, M., Schweingruber, H., Hirtzer, P., & Brandley, B. K. (1991) *Proc. Natl. Acad. Sci. U.S.A. 88*, 1138.

Tyrrell, D., James, P., Rao, N., Foxall, C., Abbas, S., Dasgupta, F., Nashed, M., Hasegawa, A., Kiso, M., Asa, D., Kidd, J., & Brandley, B. K. (1991) *Proc. Natl. Acad. Sci. U.S.A. 88*, 10372.

Urdal, D. L., Brentnall, T. A., Bernstein, I. D., & Hakomori, S.-I. (1983) *Blood 62*, 1022.

Walz, G., Aruffo, A., Kolanus, W., Bevilacqua, M., & Seed, B. (1990) *Science 250*, 1132.

Yan, Z.-Y., & Bush, C. A. (1990) *Biopolymers 29*, 799.

Yan, Z.-Y., Rao, B. N. N., & Bush, C. A. (1987) *J. Am. Chem. Soc. 109*, 7663.

Yang, H.-J., & Hakomori, S.-I. (1971) *J. Biol. Chem. 246*, 1192.